# SI Appendix

**Fig. S 1: Phenotype of p166 knockdown in BSF and γL262P cells**

A) Growth curve of *p166* RNAi BSF cells (-Tet, uninduced) and (+Tet, induced). Next to it, the cell cycle stages of the population determined by kDNA and nuclear DNA in uninduced (day 0) and induced (day 1, day 2) cells (n≥99). B) Cell growth in γL262P *p166* RNAi cells with the karyotype next to it (n≥139).

**Fig. S 2: Phenotype of p197 knockdown in BSF and γL262P cells**

A) Growth curve of *p197* RNAi BSF cells (uninduced, -Tet; induced, +Tet). Next to it, the cell cycle stages determined by kDNA and nuclear DNA in uninduced (day 0) and induced (day 1, day 2) cells (n≥100). B) Cell growth of γL262P *p197* RNAi cells for uninduced and induced with the relative occurrence of the kDNA and nucleus next to it (n≥116). C) Transmission electron microscopy pictures are shown for either *p197* RNAi induced (48h) or uninduced cells. Scale bar 2 $\mu$m D) Fluorescence microscopy of BBA4 (red) and YL1/2 (basal body, green) in *p197* RNAi cells either Tet uninduced or 2 days induced. Quantitative analyses per condition are shown next to the representative image (n≥105). Only cells with a YL1/2 signal were used for quantifications. Scale bar 3 $\mu$m.

**Fig. S 3: Depletion of p197 and investigation of the remaining TAC components by Immunofluorescence analysis**

Fluorescence microscopy images of uninduced (-Tet) or 48 h Tet induced (+Tet) *p197* RNAi cells, stained with DAPI (DNA, cyan), YL1/2 (basal body) and for each a remaining TAC protein (Mab22 (n≥98), TAC65myc (n≥117), TAC60myc (n≥86), TAC40HA (n≥96), p166PTP (n≥101), TAC102 (n≥101)) with the quantitative analysis next to it. As a control for the staining, only cells with a discernable YL1/2 signal were used. In the right panel the occurrence of the kDNA and the nucleus per staining after 0 days and 2 days of depletion. Scale bar 3 $\mu$m.

**Fig. S 4: Depletion of TAC65 and investigation of the remaining TAC components by Immunofluorescence analysis**

Fluorescence microscopy images of uninduced (-Tet) or 48 h Tet induced (+Tet) *TAC65* RNAi cells, stained with DAPI (DNA, cyan), BBA4 or YL1/2 (basal body) and for each a remaining TAC protein (p197PTP (n≥88), Mab22 (n≥88), TAC60 (n≥106), TAC40HA (n≥77), p166PTP (n≥94), TAC102 (n≥98)) with the quantitative analysis next to it. As a control for the staining, only cells with a discernable BBA4 or YL1/2 signal were used. In the right panel the occurrence of the kDNA and the nucleus per staining after 0 days and 2 days of depletion. Scale bar 3 $\mu$m.

**Fig. S 5: Depletion of TAC60 and investigation of the remaining TAC components by Immunofluorescence analysis**

Fluorescence microscopy images of uninduced (-Tet) or 48 h Tet induced (+Tet) *TAC60* RNAi cells, stained with DAPI (DNA, cyan), BBA4 or YL1/2 (basal body) and for each a remaining TAC protein (p197PTP (n≥102), Mab22 (n≥96), TAC65myc (n≥83), TAC40HA (n≥93), p166PTP (n≥110), TAC102 (n≥114)) with the quantitative analysis next to it. As a control for the staining, only cells with a discernable BBA4 or YL1/2 signal were used. In the right panel the occurrence of the kDNA and the nucleus per staining after 0 days and 2 days of depletion. Scale bar 3 $\mu$m.

**Fig. S 6: Depletion of TAC40 and investigation of the remaining TAC components by Immunofluorescence analysis**

Fluorescence microscopy images of uninduced (-Tet) or 48 h Tet induced (+Tet) *TAC40* RNAi cells, stained with DAPI (DNA, cyan), BBA4 or YL1/2 (basal body) and for each a remaining TAC protein (p197PTP (n≥98), Mab22 (n≥108), TAC65myc (n≥97), TAC60myc (n≥92), p166PTP (n=112), TAC102 (n≥93)) with the quantitative analysis next to it. As a control for the staining, only cells with a discernable BBA4 or YL1/2 signal were used. In the right panel the occurrence of the kDNA and the nucleus per staining after 0 days and 2 days of depletion. Scale bar 3 $\mu$m.

**Fig. S 7: Depletion of p166 and investigation of the remaining TAC components by Immunofluorescence analysis**

Fluorescence microscopy images of uninduced (-Tet) or 48 h Tet induced (+Tet) *p166* RNAi cells, stained with DAPI (DNA, cyan), BBA4 or YL1/2 (basal body) and for each a remaining TAC protein (p197PTP (n≥89), Mab22 (n≥110), TAC65myc (n≥107), TAC60myc (n≥103), TAC40HA (n≥101), TAC102 (n≥90)) with the quantitative analysis next to it. As a control for the staining, only cells with a discernable BBA4 or YL1/2 signal were used. In the right panel the occurrence of the kDNA and the nucleus per staining after 0 days and 2 days of depletion. Scale bar 3 $\mu$m.

**Fig. S 8: Depletion of TAC102 and investigation of the remaining TAC components by Immunofluorescence analysis**

Fluorescence microscopy images of uninduced (-Tet) or 48 h Tet induced (+Tet) *TAC102* RNAi cells, stained with DAPI (DNA, cyan), BBA4 or YL1/2 (basal body) and for each a remaining TAC protein (p197PTP (n=101), Mab22 (n≥97), TAC65myc (n≥105), TAC60 (n≥104), TAC40HA (n≥99), p166PTP (n≥97)) with the quantitative analysis next to it. As a control for the staining, only cells with a discernable BBA4 or YL1/2 signal were used. In the right panel the occurrence of the kDNA and the nucleus per staining after 0 days and 2 days of depletion. Scale bar 3 $\mu$m.

**Fig. S 9: Depletion of p197 and investigation of TAC components by western blot analysis**
Protein abundance of TAC65myc (n=3), TAC60myc (n=3), TAC40HA (n=3), p166PTP (n=3) and TAC102 (n=6) determined by western blotting from cells uninduced, 24 h or 48 h post *p197* RNAi induction. Next to it, quantification of the protein abundance. ATOM40 abundance was used as a loading control.

**Fig. S 10: Depletion of TAC65 and investigation of TAC components by western blot analysis**
Protein abundance of TAC40HA (n=3), p166PTP (n=3) and TAC102 (n=6) determined by western blotting from cells uninduced, 24 h or 48 h post *TAC65* RNAi induction. Next to it, quantification of the protein abundance. ATOM40 abundance was used as a loading control.

**Fig. S 11: Depletion of TAC60 and investigation of TAC components by western blot analysis**
Protein abundance of TAC65myc (n=3), TAC40HA (n=3), p166PTP (n=3) and TAC102 (n=6) determined by western blotting from cells uninduced, 24 h or 48 h post *TAC60* RNAi induction. Next to it, quantification of the protein abundance. ATOM40 abundance was used as a loading control. Calculating the p-value by two-tailed heteroscedastic t-test performed significance measurements (* $p \leq 0.05$; ** $p < 0.01$; *** $p < 0.001$; **** $p < 0.0001$).

**Fig. S 12: Depletion of TAC40 and investigation of TAC components by western blot analysis**
Protein abundance of TAC65myc (n=3), TAC60myc (n=3), p166PTP (n=3) and TAC102 (n=3) determined by western blotting from cells uninduced, 24 h or 48 h post *TAC40* RNAi induction. Next to it, quantification of the protein abundance. ATOM40 abundance was used as a loading control.

**Fig. S 13: Depletion of p166 and investigation of TAC components by western blot analysis**
Protein abundance TAC102 (n=3) determined by western blotting from cells uninduced, 24 h or 48 h post *p166* RNAi induction. Next to it, quantification of the protein abundance. ATOM40 abundance was used as a loading control. Calculating the p-value by two-tailed heteroscedastic t-test performed significance measurements (* $p \leq 0.05$; ** $p < 0.01$; *** $p < 0.001$; **** $p < 0.0001$).

**Fig. S 14: Complex formation of TAC60 on blue native PAGE**

Western blot from blue native PAGE of mitochondrial protein fraction of BSF cells probed with myc for TAC60myc or anti-ATOM40 in *p197* RNAi uninduced and induced cells (day 0 and day 2).

**Fig. S 15: TAC biogenesis after recovery from p166 depletion**

A) Growth curve of γL262P *p166* RNAi cells. After 5 days of *p166* RNAi induction, cells were washed and grown in medium without Tet. .B) Percentage of cells with kDNA and nucleus in *p166* RNAi induced and uninduced trypanosomes (n≥95). C) TAC102 (green), YL1/2 (red) for the basal body and DAPI (cyan) for the DNA stained cells after 0 and 5 days of Tet induction (post induction p.i.) and two days post recovery (p.r.) are shown. D) Quantitative analysis of TAC102 (n≥112) or Mab22 (n≥95) in uninduced (-Tet), 5 days induced (5d p.i.) and 1 or 2 days after removing Tet (1d p.r., 2d p.r.) in γL262P *p166* RNAi cells. As a control for the staining, only cells with a discernable basal body signal were used. A black bar indicates a correct localized signal; a grey bar indicates a weak signal and a light grey a mislocalized signal. Scale bar 3 $\mu$m.

**Fig. S 16: Dynamics of the TAC proteins during the kDNA replication**

Tagged BSF cells were stained with DAPI (DNA, cyan), BBA4 (red), anti-HA for TAC40HA (yellow) and anti-ProteinA for TAC102PTP (green). All 125 cells are shown and grouped according to the number of signals. The first number indicates BBA4, the second TAC40, the third TAC102 and the fourth the kDNA. Other possibilities than 1-1-1-1, 2-1-1-1, 2-2-1-1 and 2-2-2-1 are summarized as others.

**Fig S1**

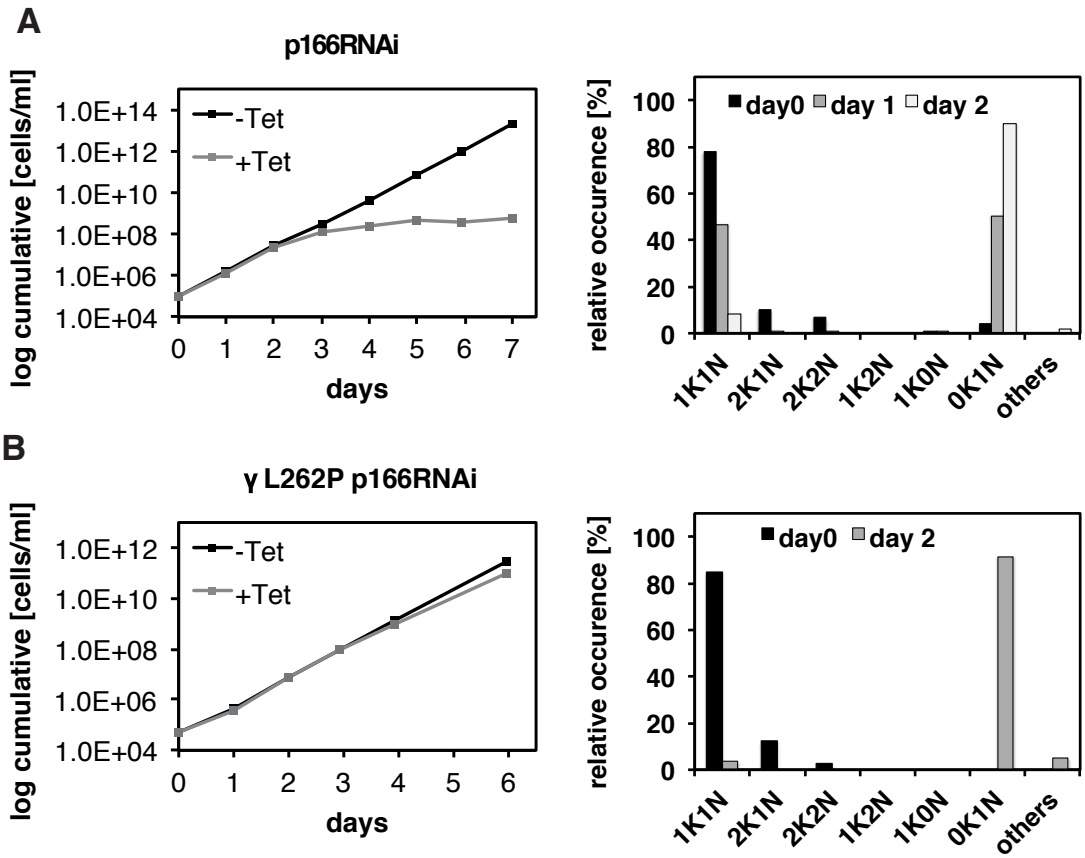
A
p166RNAi
log cumulative [cells/ml]
1.0E+14
1.0E+12
1.0E+10
1.0E+08
1.0E+06
1.0E+04
-Tet
+Tet
0 1 2 3 4 5 6 7
days
relative occurence [%]
100
80
60
40
20
0
day0 day 1 day 2
1K1N 2K1N 2K2N 1K2N 1K0N 0K1N others
B
γ L262P p166RNAi
log cumulative [cells/ml]
1.0E+12
1.0E+10
1.0E+08
1.0E+06
1.0E+04
-Tet
+Tet
0 1 2 3 4 5 6
days
relative occurence [%]
100
80
60
40
20
0
day0 day 2
1K1N 2K1N 2K2N 1K2N 1K0N 0K1N others

Fig S2

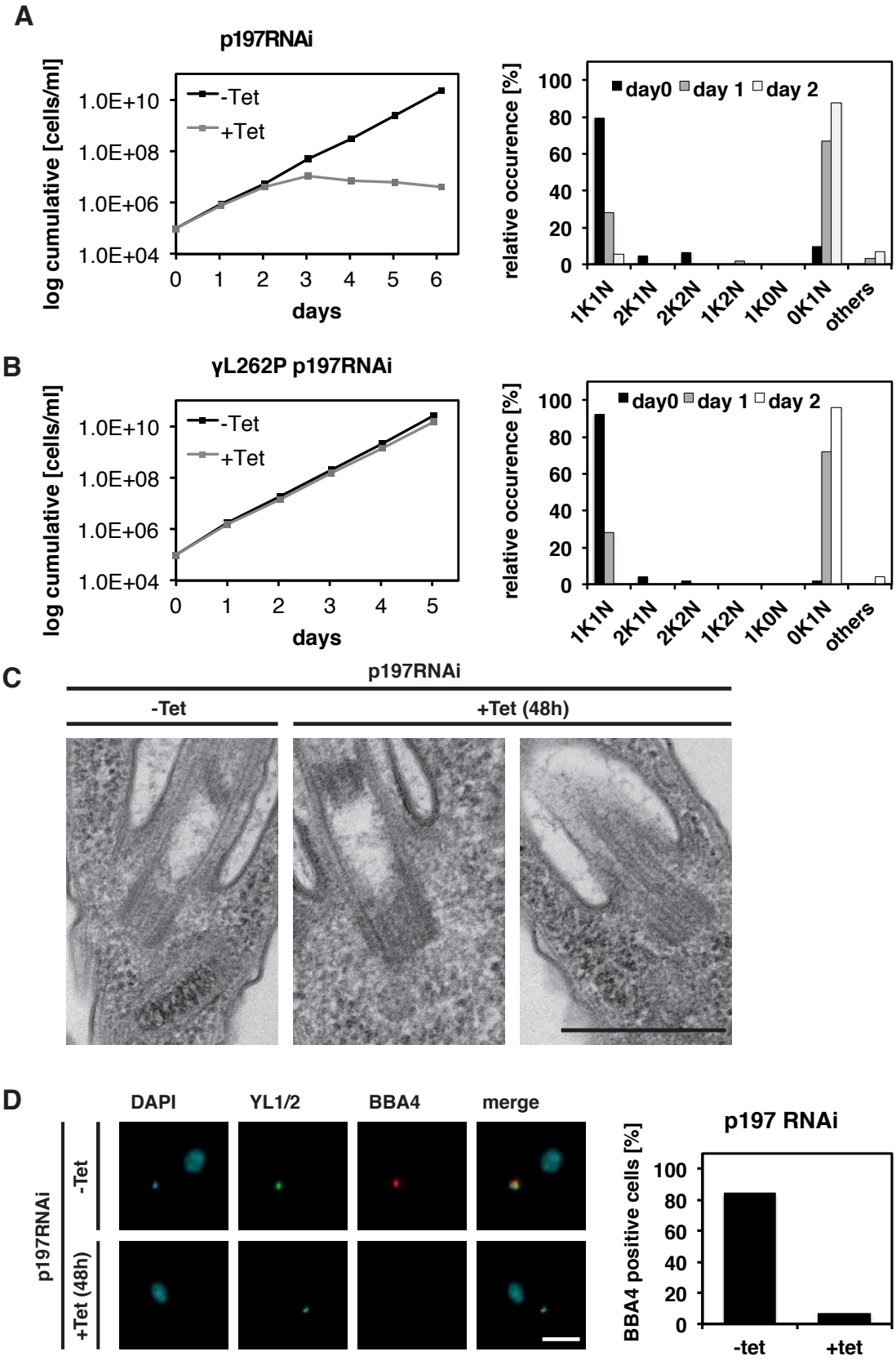
A
p197RNAi
log cumulative [cells/ml]
1.0E+10
1.0E+08
1.0E+06
1.0E+04
-Tet
+Tet
0 1 2 3 4 5 6
days
relative occurence [%]
day0 day 1 day 2
100 80 60 40 20 0
1K1N 2K1N 2K2N 1K2N 1K0N 0K1N others
B
γL262P p197RNAi
log cumulative [cells/ml]
1.0E+10
1.0E+08
1.0E+06
1.0E+04
-Tet
+Tet
0 1 2 3 4 5
days
relative occurence [%]
day0 day 1 day 2
100 80 60 40 20 0
1K1N 2K1N 2K2N 1K2N 1K0N 0K1N others
C
p197RNAi
-Tet
+Tet (48h)
D
DAPI
YL1/2
BBA4
merge
p197RNAi
-Tet
+Tet (48h)
p197 RNAi
BBA4 positive cells [%]
100 80 60 40 20 0
-tet
+tet

Fig S3

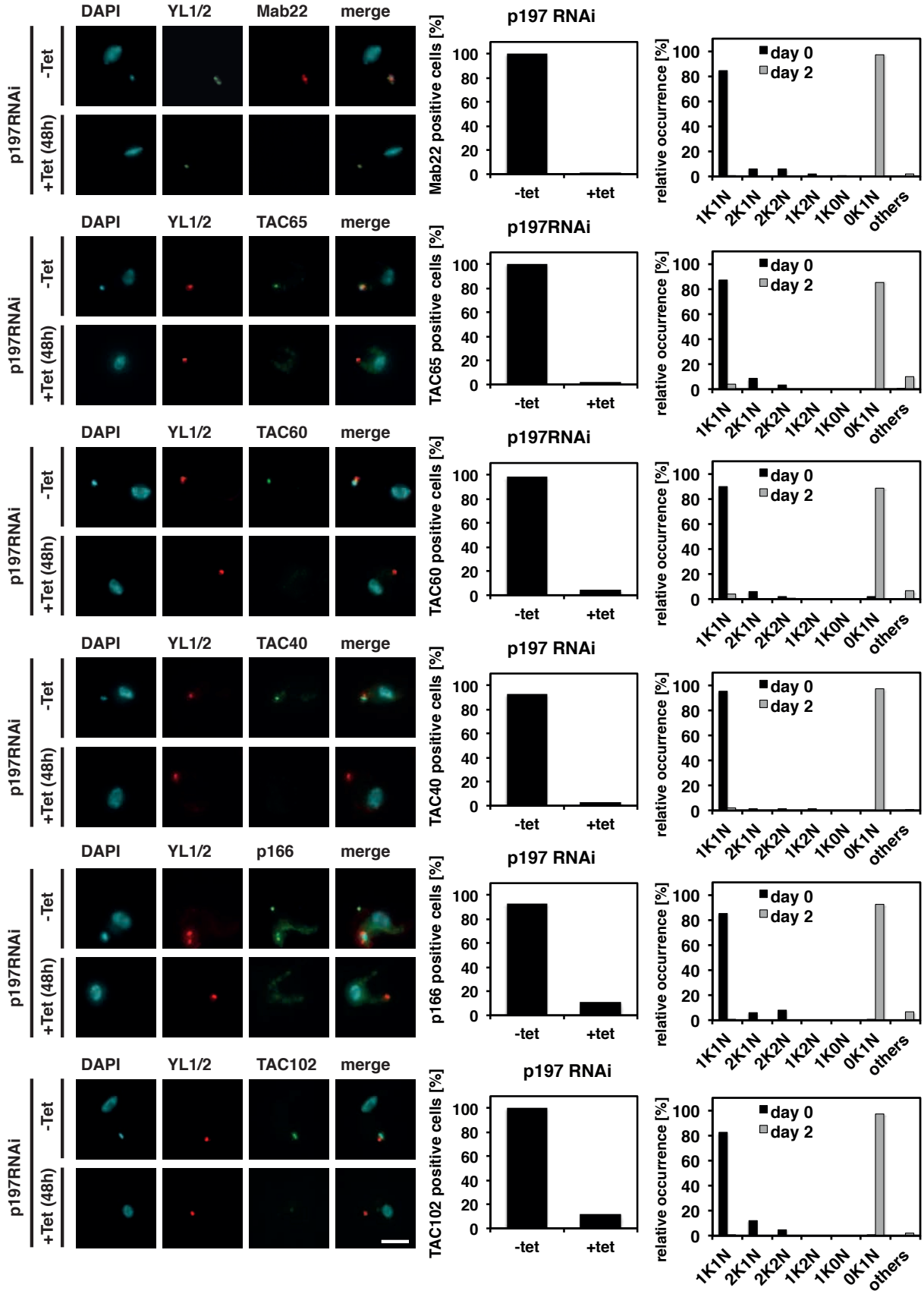
DAPI
YL1/2
Mab22
merge
p197RNAi
-Tet
+Tet (48h)
p197 RNAi
Mab22 positive cells [%]
-tet
+tet
relative occurrence [%]
day 0
day 2
1K1N
2K1N
2K2N
1K2N
1K0N
0K1N
others
TAC65
p197RNAi
TAC65 positive cells [%]
TAC60
TAC60 positive cells [%]
TAC40
TAC40 positive cells [%]
p166
p166 positive cells [%]
TAC102
TAC102 positive cells [%]

Fig S4

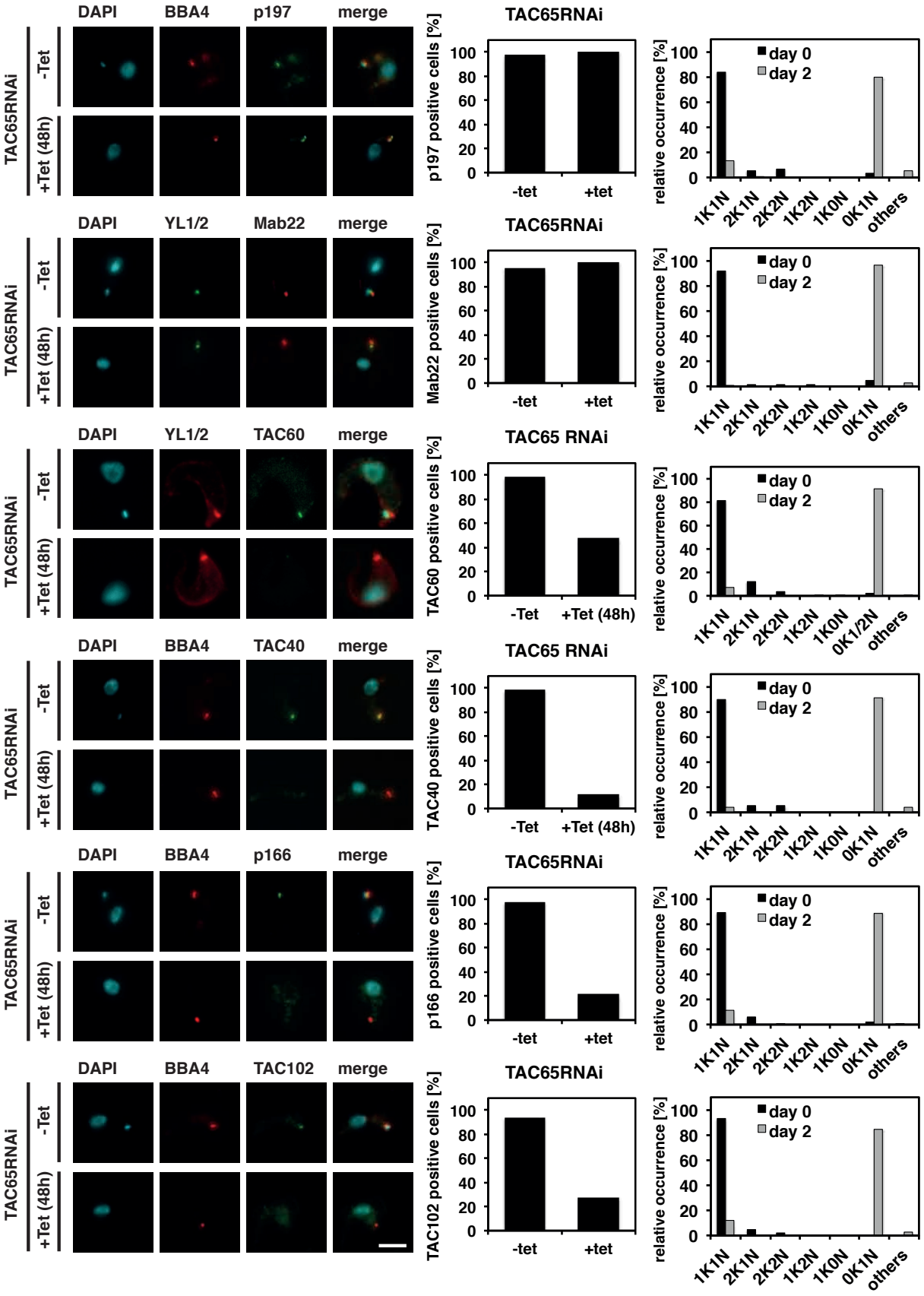
DAPI
BBA4
p197
merge
TAC65RNAi
-Tet
+Tet (48h)
TAC65RNAi
p197 positive cells [%]
-tet
+tet
relative occurrence [%]
day 0
day 2
1K1N
2K1N
2K2N
1K2N
1K0N
0K1N
others
DAPI
YL1/2
Mab22
merge
Mab22 positive cells [%]
DAPI
YL1/2
TAC60
merge
TAC60 positive cells [%]
TAC65 RNAi
-Tet
+Tet (48h)
0K1/2N
DAPI
BBA4
TAC40
merge
TAC40 positive cells [%]
DAPI
BBA4
p166
merge
p166 positive cells [%]
DAPI
BBA4
TAC102
merge
TAC102 positive cells [%]

Fig S5

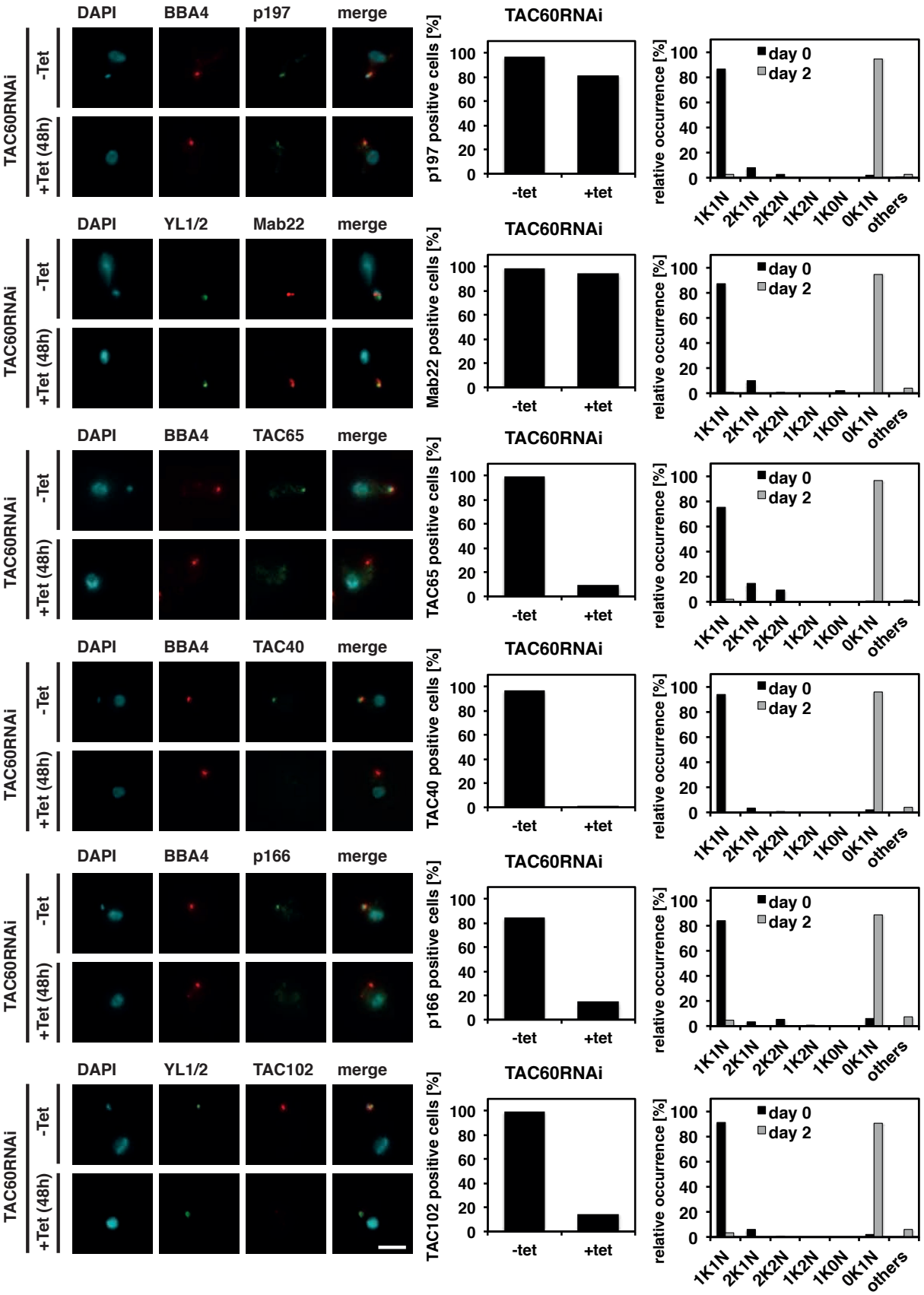
DAPI
BBA4
p197
merge
TAC60RNAi
-Tet
+Tet (48h)
TAC60RNAi
p197 positive cells [%]
-tet
+tet
relative occurrence [%]
day 0
day 2
1K1N
2K1N
2K2N
1K2N
1K0N
0K1N
others
DAPI
YL1/2
Mab22
merge
Mab22 positive cells [%]
DAPI
BBA4
TAC65
merge
TAC65 positive cells [%]
DAPI
BBA4
TAC40
merge
TAC40 positive cells [%]
DAPI
BBA4
p166
merge
p166 positive cells [%]
DAPI
YL1/2
TAC102
merge
TAC102 positive cells [%]

Fig S6

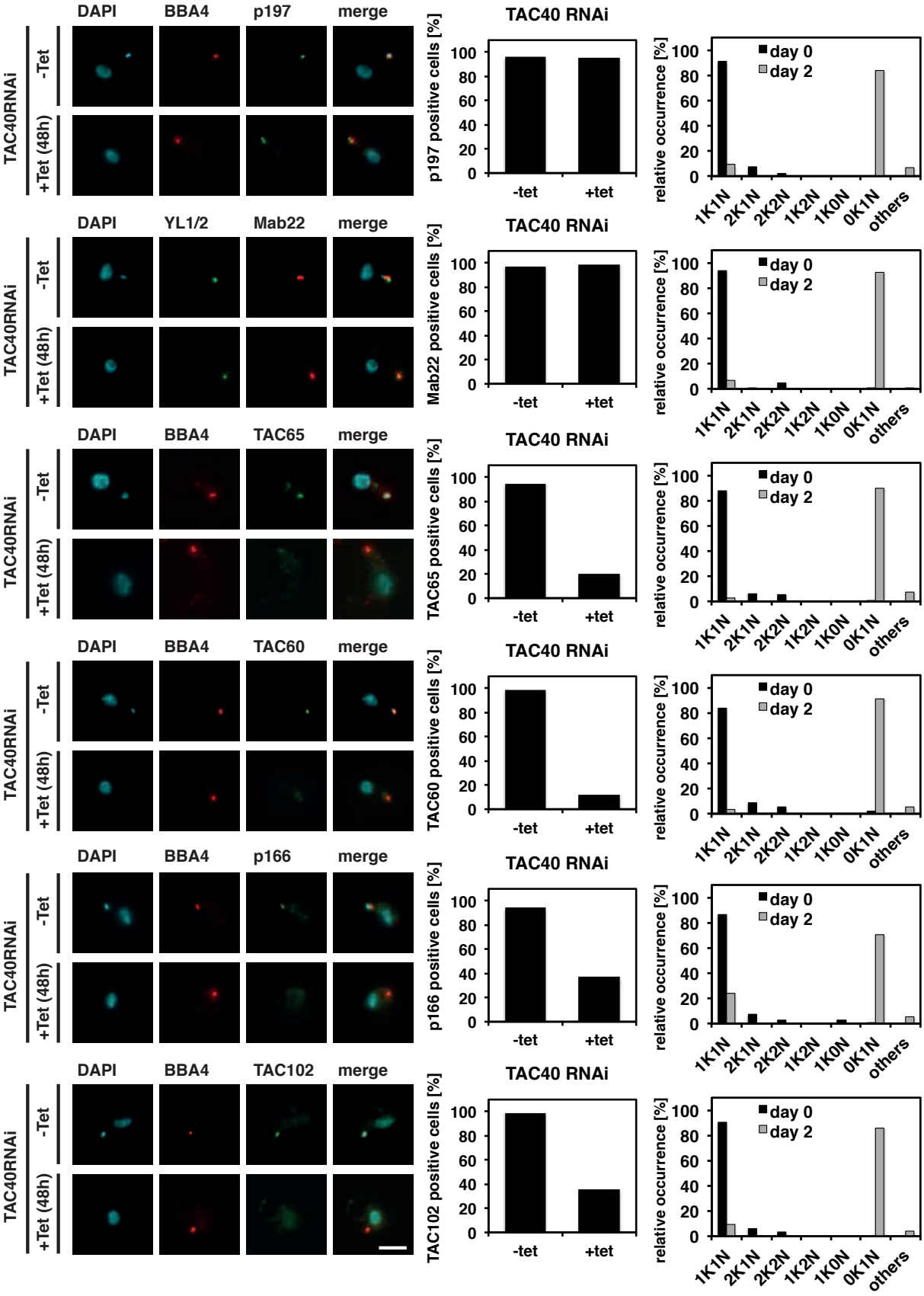
DAPI
BBA4
p197
merge
TAC40RNAi
-Tet
+Tet (48h)
TAC40 RNAi
p197 positive cells [%]
-tet
+tet
relative occurrence [%]
day 0
day 2
1K1N
2K1N
2K2N
1K2N
1K0N
0K1N
others
DAPI
YL1/2
Mab22
merge
Mab22 positive cells [%]
DAPI
BBA4
TAC65
merge
TAC65 positive cells [%]
DAPI
BBA4
TAC60
merge
TAC60 positive cells [%]
DAPI
BBA4
p166
merge
p166 positive cells [%]
DAPI
BBA4
TAC102
merge
TAC102 positive cells [%]

Fig S7

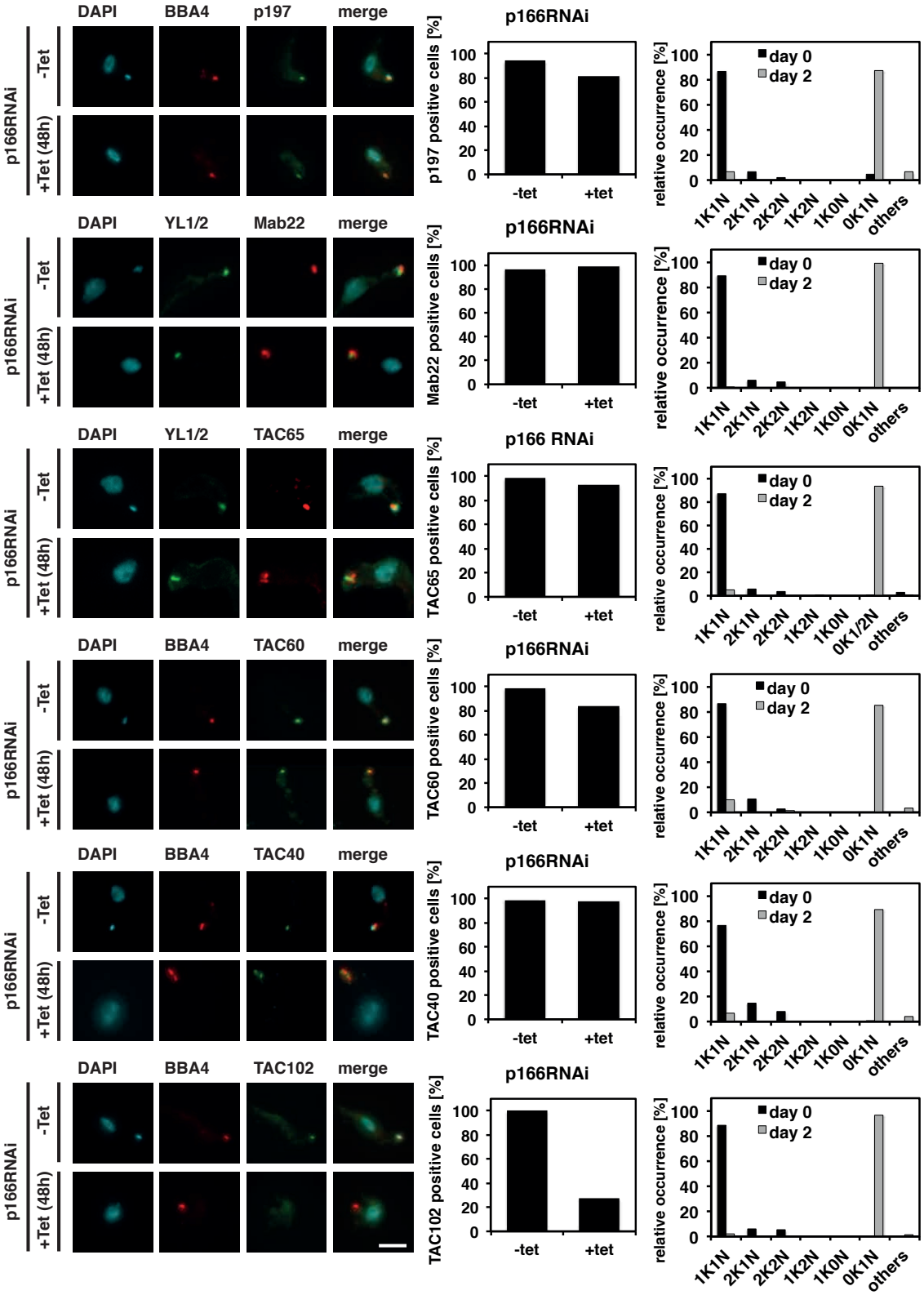
DAPI
BBA4
p197
merge
p166RNAi
-Tet
+Tet (48h)
p166RNAi
p197 positive cells [%]
-tet
+tet
relative occurrence [%]
day 0
day 2
1K1N
2K1N
2K2N
1K2N
1K0N
0K1N
others
DAPI
YL1/2
Mab22
merge
Mab22 positive cells [%]
DAPI
YL1/2
TAC65
merge
p166 RNAi
TAC65 positive cells [%]
0K1/2N
DAPI
BBA4
TAC60
merge
TAC60 positive cells [%]
DAPI
BBA4
TAC40
merge
TAC40 positive cells [%]
DAPI
BBA4
TAC102
merge
TAC102 positive cells [%]

Fig S8

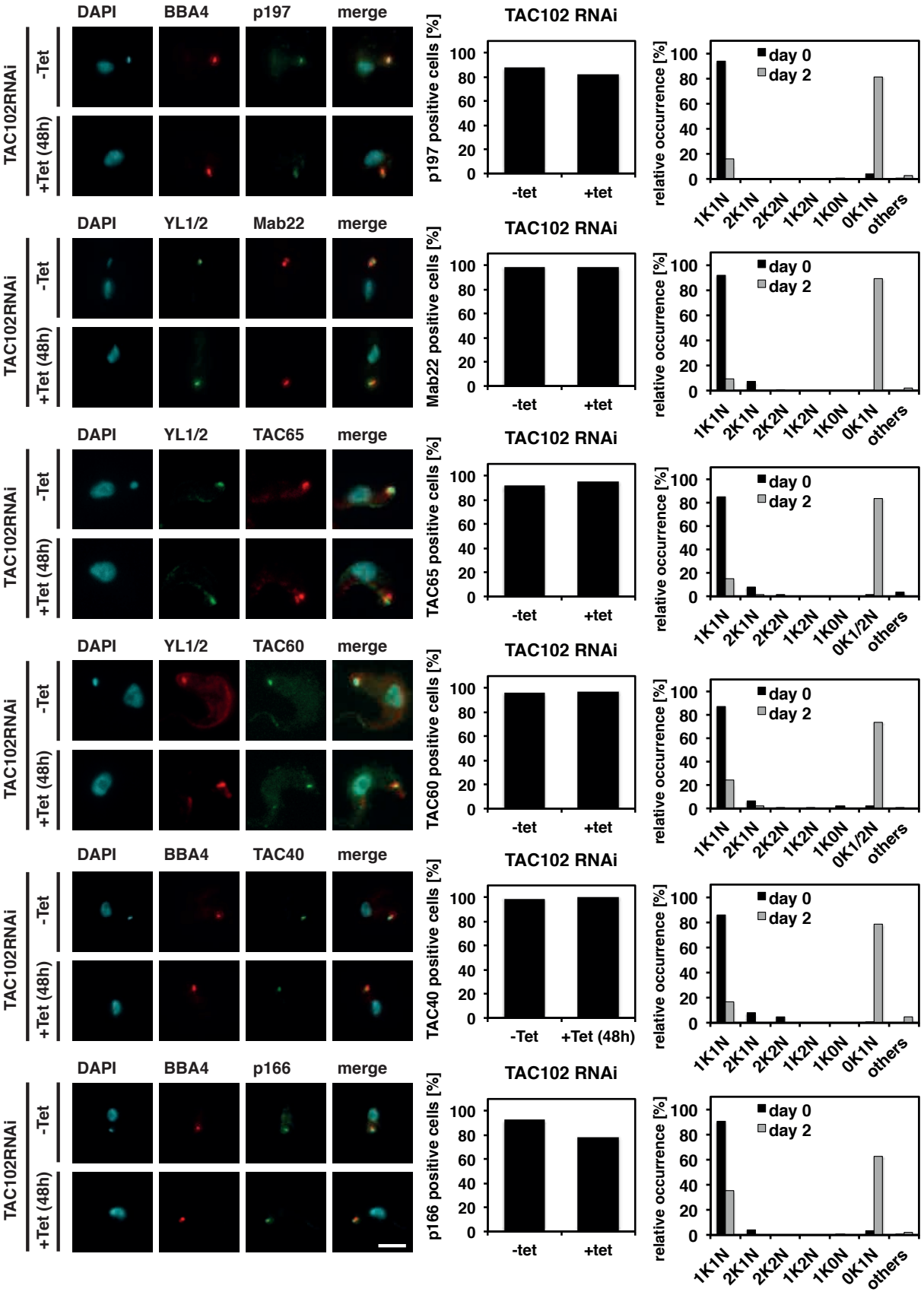
DAPI
BBA4
p197
merge
TAC102RNAi
-Tet
+Tet (48h)
TAC102 RNAi
p197 positive cells [%]
-tet
+tet
relative occurrence [%]
day 0
day 2
1K1N
2K1N
2K2N
1K2N
1K0N
0K1N
others
DAPI
YL1/2
Mab22
merge
Mab22 positive cells [%]
DAPI
YL1/2
TAC65
merge
TAC65 positive cells [%]
0K1/2N
DAPI
YL1/2
TAC60
merge
TAC60 positive cells [%]
DAPI
BBA4
TAC40
merge
TAC40 positive cells [%]
DAPI
BBA4
p166
merge
p166 positive cells [%]

Fig S9

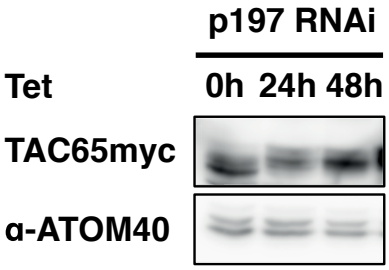
p197 RNAi
Tet
0h 24h 48h
TAC65myc
α-ATOM40

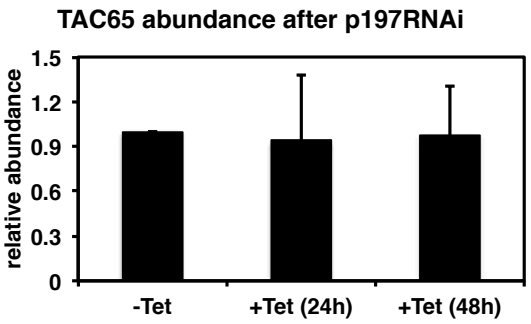
TAC65 abundance after p197RNAi
relative abundance
1.5
1.2
0.9
0.6
0.3
0
-Tet
+Tet (24h)
+Tet (48h)

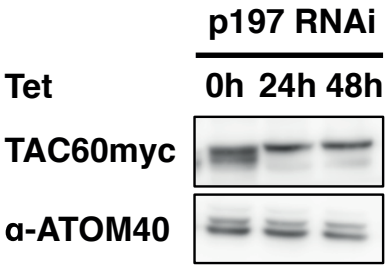
p197 RNAi
Tet
0h 24h 48h
TAC60myc
α-ATOM40

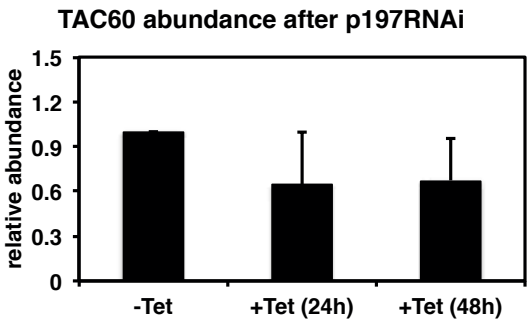
TAC60 abundance after p197RNAi
relative abundance
1.5
1.2
0.9
0.6
0.3
0
-Tet
+Tet (24h)
+Tet (48h)

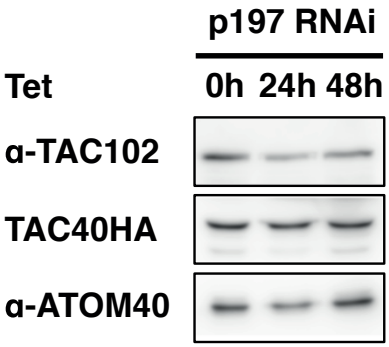
p197 RNAi
Tet
0h 24h 48h
α-TAC102
TAC40HA
α-ATOM40

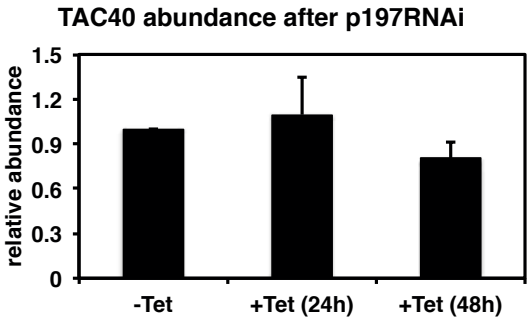
TAC40 abundance after p197RNAi
relative abundance
1.5
1.2
0.9
0.6
0.3
0
-Tet
+Tet (24h)
+Tet (48h)

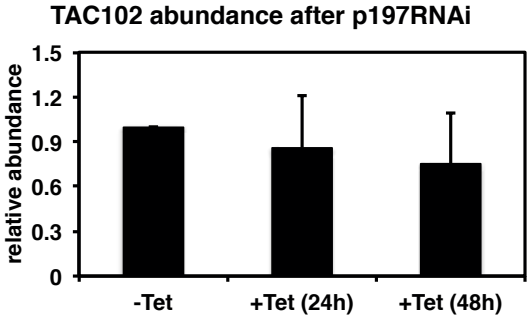
TAC102 abundance after p197RNAi
relative abundance
1.5
1.2
0.9
0.6
0.3
0
-Tet
+Tet (24h)
+Tet (48h)

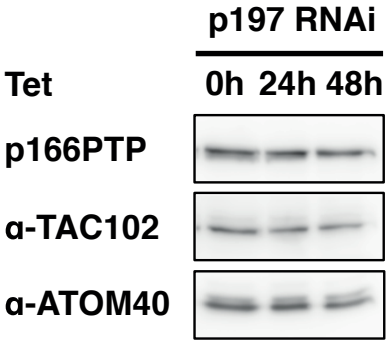
p197 RNAi
Tet
0h 24h 48h
p166PTP
α-TAC102
α-ATOM40

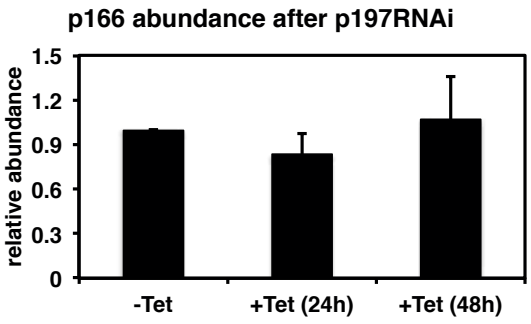
p166 abundance after p197RNAi
relative abundance
1.5
1.2
0.9
0.6
0.3
0
-Tet
+Tet (24h)
+Tet (48h)

Fig S10

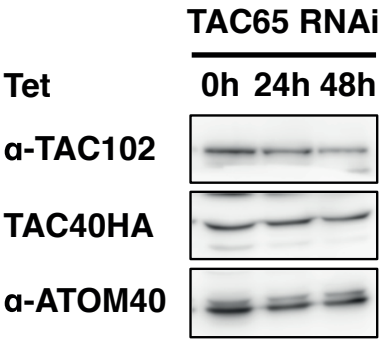
TAC65 RNAi
Tet
0h 24h 48h
α-TAC102
TAC40HA
α-ATOM40

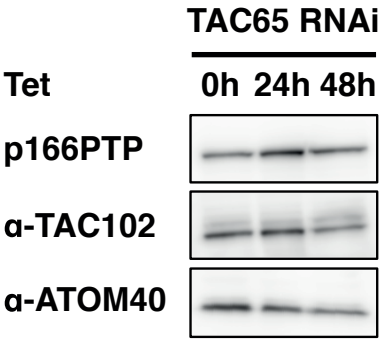
TAC65 RNAi
Tet
0h 24h 48h
p166PTP
α-TAC102
α-ATOM40

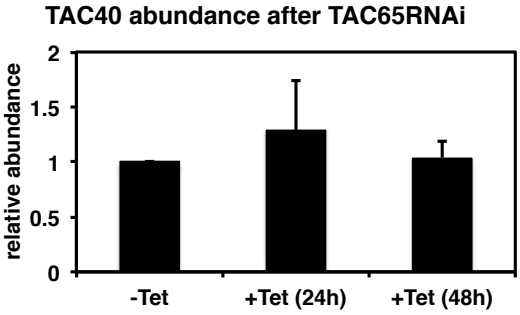
TAC40 abundance after TAC65RNAi
relative abundance
2
1.5
1
0.5
0
-Tet
+Tet (24h)
+Tet (48h)

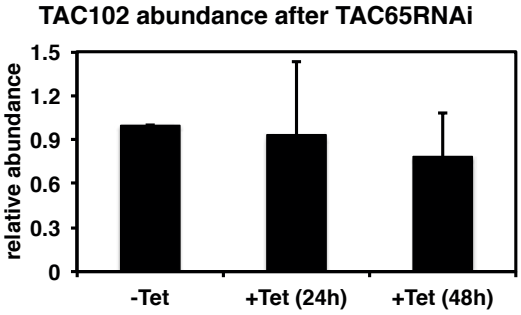
TAC102 abundance after TAC65RNAi
relative abundance
1.5
1.2
0.9
0.6
0.3
0
-Tet
+Tet (24h)
+Tet (48h)

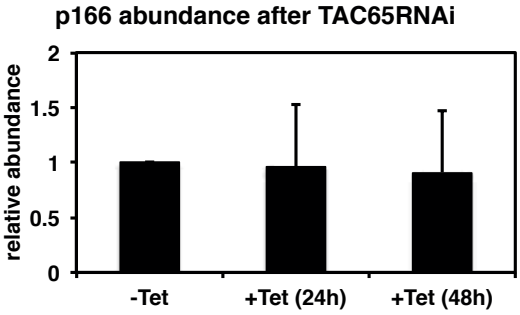
p166 abundance after TAC65RNAi
relative abundance
2
1.5
1
0.5
0
-Tet
+Tet (24h)
+Tet (48h)

Fig S11

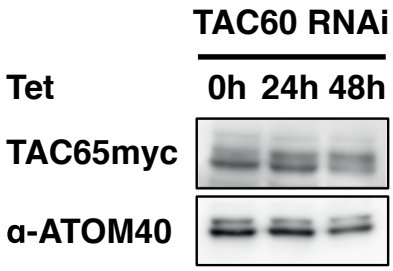
TAC60 RNAi
Tet
0h 24h 48h
TAC65myc
α-ATOM40

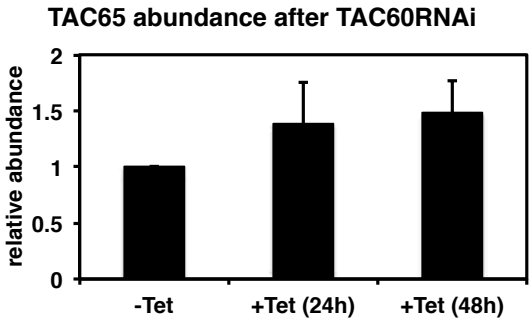
TAC65 abundance after TAC60RNAi
relative abundance
2
1.5
1
0.5
0
-Tet
+Tet (24h)
+Tet (48h)

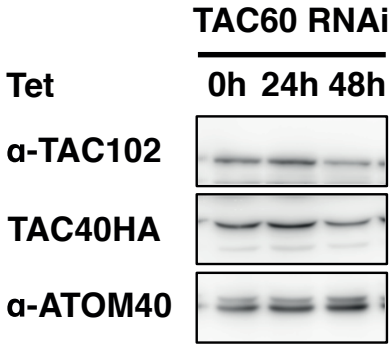
TAC60 RNAi
Tet
0h 24h 48h
α-TAC102
TAC40HA
α-ATOM40

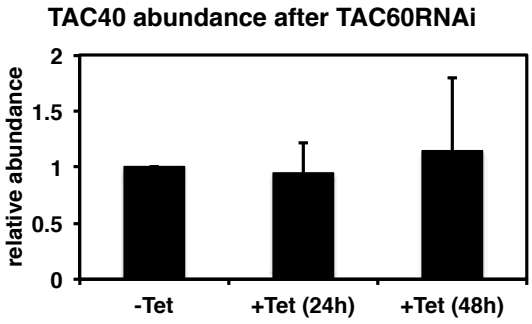
TAC40 abundance after TAC60RNAi
relative abundance
2
1.5
1
0.5
0
-Tet
+Tet (24h)
+Tet (48h)

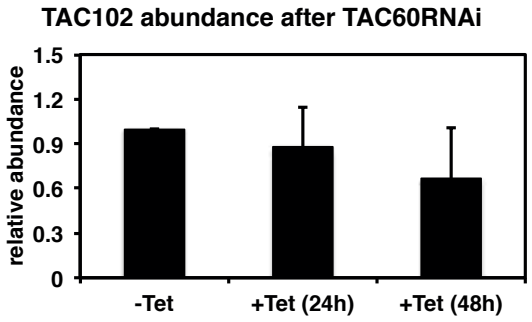
TAC102 abundance after TAC60RNAi
relative abundance
1.5
1.2
0.9
0.6
0.3
0
-Tet
+Tet (24h)
+Tet (48h)

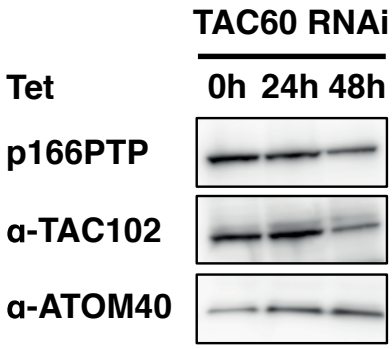
TAC60 RNAi
Tet
0h 24h 48h
p166PTP
α-TAC102
α-ATOM40

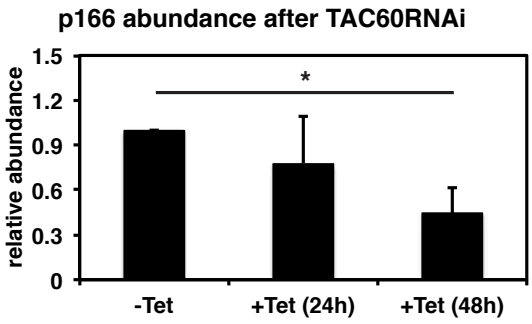
p166 abundance after TAC60RNAi
relative abundance
1.5
1.2
0.9
0.6
0.3
0
*
-Tet
+Tet (24h)
+Tet (48h)

Fig S12

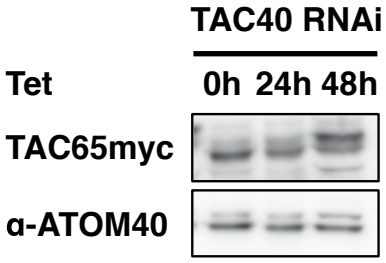
TAC40 RNAi
Tet
0h 24h 48h
TAC65myc
α-ATOM40

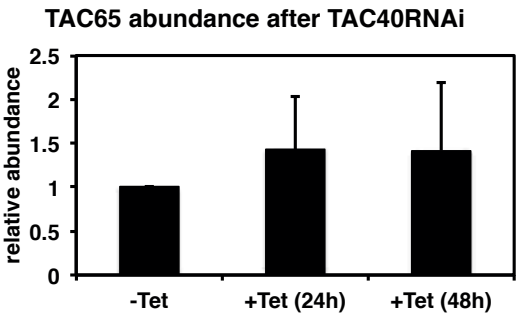
TAC65 abundance after TAC40RNAi
relative abundance
2.5
2
1.5
1
0.5
0
-Tet
+Tet (24h)
+Tet (48h)

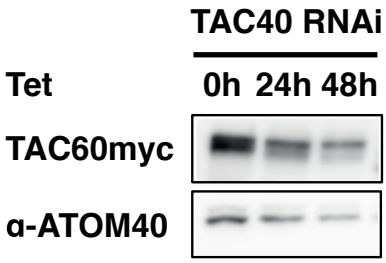
TAC40 RNAi
Tet
0h 24h 48h
TAC60myc
α-ATOM40

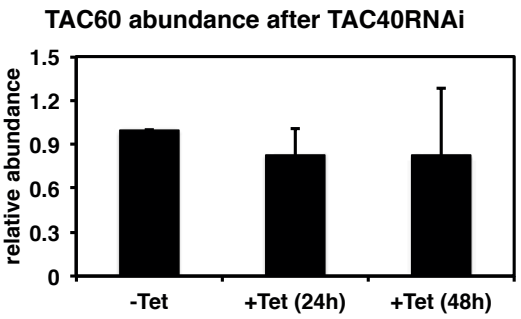
TAC60 abundance after TAC40RNAi
relative abundance
1.5
1.2
0.9
0.6
0.3
0
-Tet
+Tet (24h)
+Tet (48h)

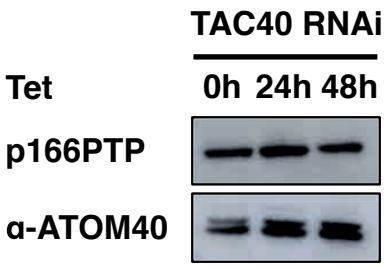
TAC40 RNAi
Tet
0h 24h 48h
p166PTP
α-ATOM40

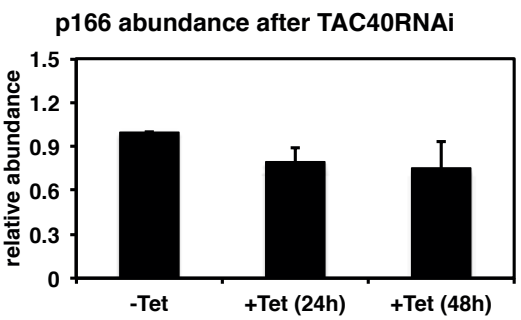
p166 abundance after TAC40RNAi
relative abundance
1.5
1.2
0.9
0.6
0.3
0
-Tet
+Tet (24h)
+Tet (48h)

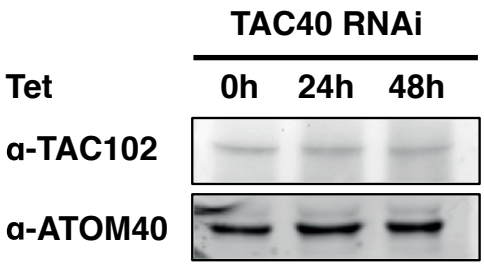
TAC40 RNAi
Tet
0h 24h 48h
α-TAC102
α-ATOM40

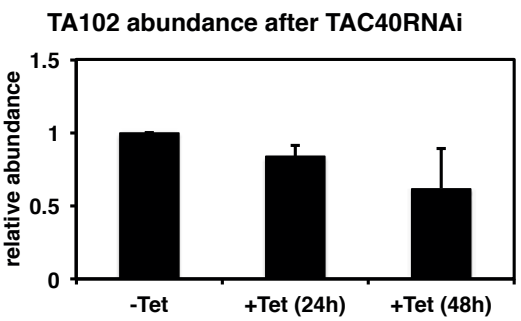
TA102 abundance after TAC40RNAi
relative abundance
1.5
1
0.5
0
-Tet
+Tet (24h)
+Tet (48h)

Fig S13

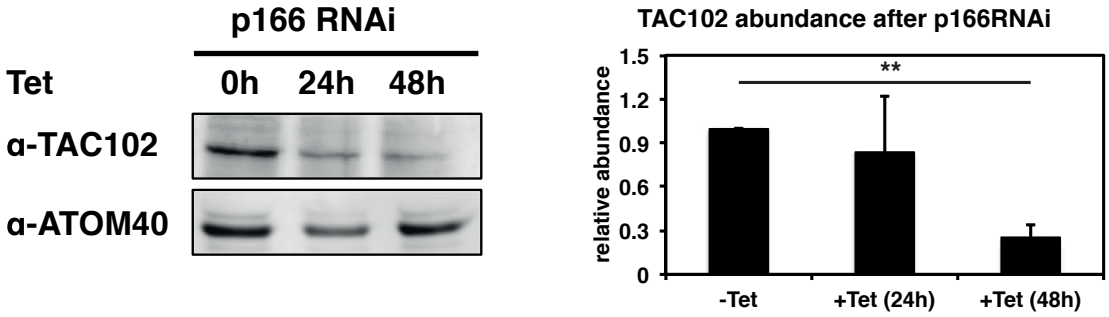


Fig S14

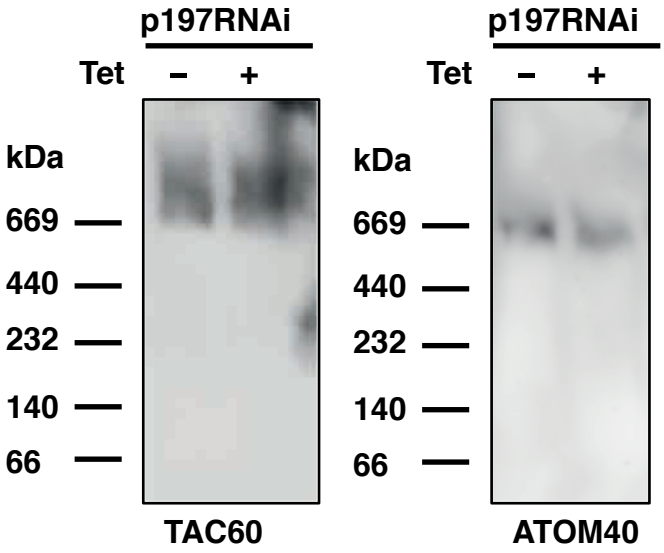

Fig S15

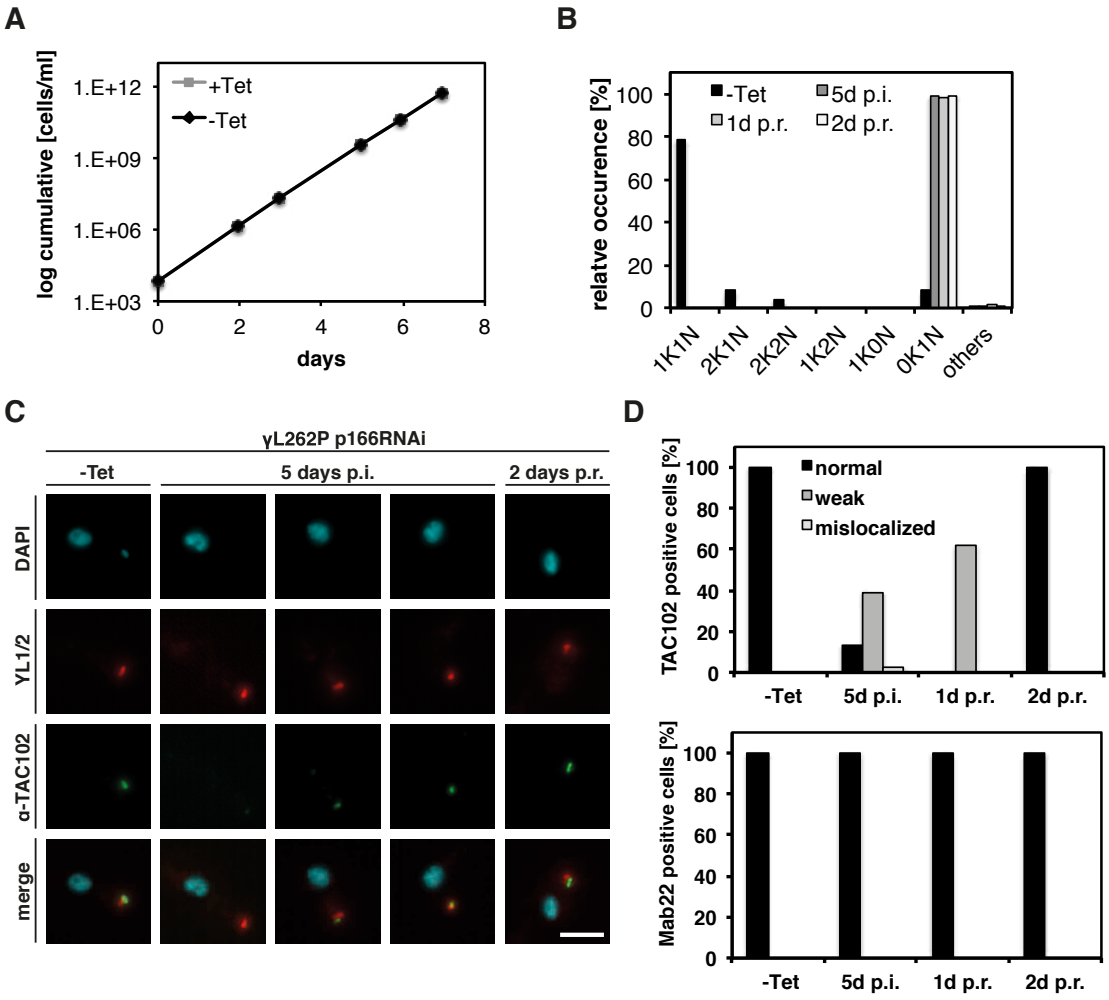
A
log cumulative [cells/ml]
1.E+12
1.E+09
1.E+06
1.E+03
+Tet
-Tet
0
2
4
6
8
days
B
relative occurence [%]
100
80
60
40
20
0
-Tet
5d p.i.
1d p.r.
2d p.r.
1K1N
2K1N
2K2N
1K2N
1K0N
0K1N
others
C
γL262P p166RNAi
-Tet
5 days p.i.
2 days p.r.
DAPI
YL1/2
α-TAC102
merge
D
TAC102 positive cells [%]
normal
weak
mislocalized
-Tet
5d p.i.
1d p.r.
2d p.r.
Mab22 positive cells [%]

Fig S16

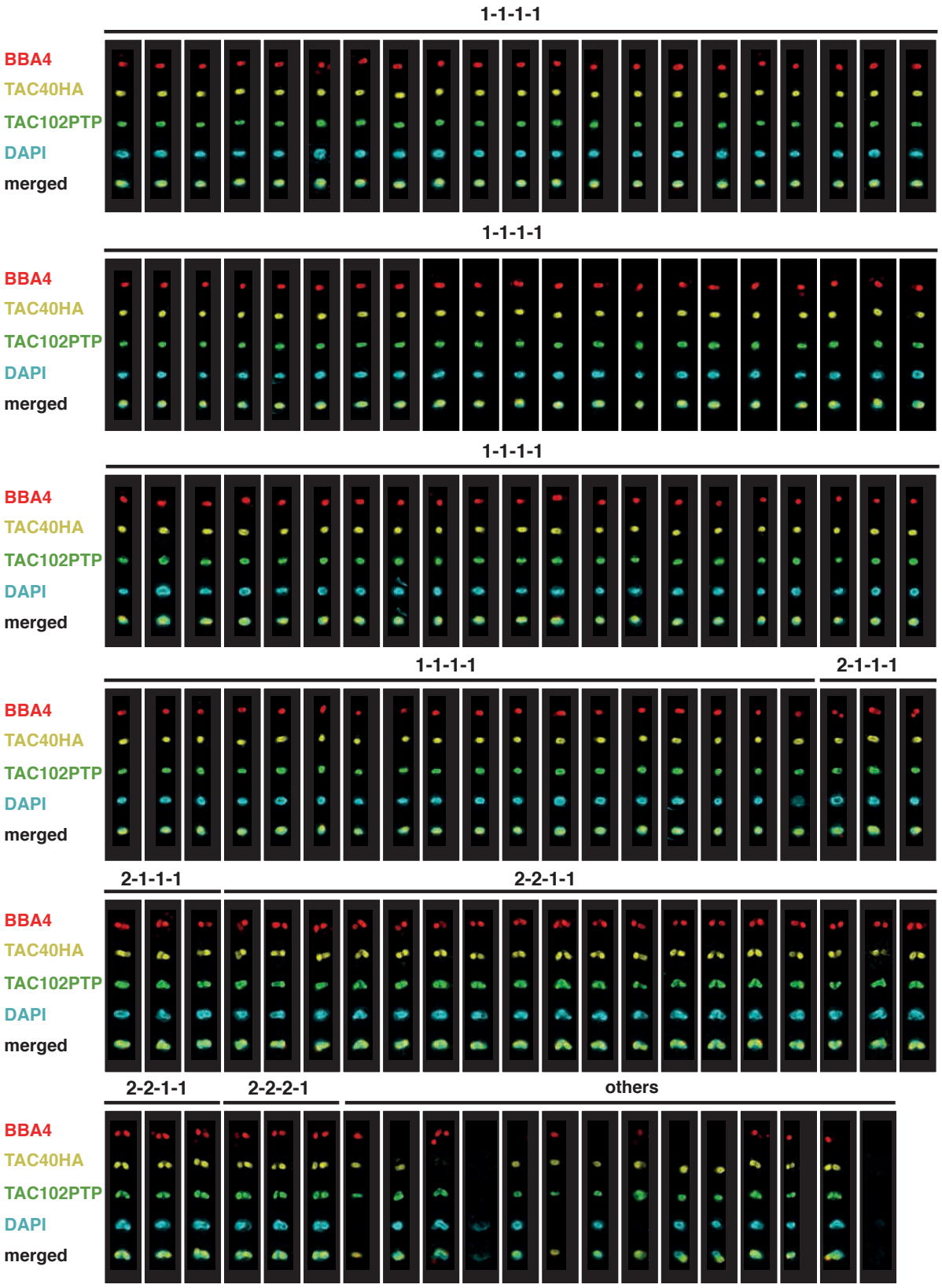
1-1-1-1
BBA4
TAC40HA
TAC102PTP
DAPI
merged
1-1-1-1
BBA4
TAC40HA
TAC102PTP
DAPI
merged
1-1-1-1
BBA4
TAC40HA
TAC102PTP
DAPI
merged
1-1-1-1
2-1-1-1
BBA4
TAC40HA
TAC102PTP
DAPI
merged
2-1-1-1
2-2-1-1
BBA4
TAC40HA
TAC102PTP
DAPI
merged
2-2-1-1
2-2-2-1
others
BBA4
TAC40HA
TAC102PTP
DAPI
merged

**Table S1: TAC orthologs**

| Organism | TAC102 | p166 | TAC40 | TAC60 | TAC65 | p197 |
|---|---|---|---|---|---|---|
| *Blechomonas ayalai* B08-376 | X | X | X | X | X | X |
| *Crithidia fasciculata* strain Cf-Cl | X | X | X | X | X | X |
| *Endotrypanum monterogeii* strain LV88 | X | X | X | X | X | X |
| *Leishmania aethiopica* L147 | X | X | X | X | X | X |
| *Leishmania amazonensis* MHOM/BR/71973/M2269 | | | | | | |
| *Leishmania arabica* strain LEM1108 | X | X | X | X | X | X |
| *Leishmania braziliensis* MHOM/BR/75/M2903 | X | X | X | X | X | X |
| *Leishmania braziliensis* MHOM/BR/75/M2904 | X | X | X | X | X | X |
| *Leishmania donovani* BPK282A1 | X | X | X | X | X | X |
| *Leishmania donovani* strain BHU 1220 | | | | | | |
| *Leishmania enriettii* strain LEM3045 | X | X | X | X | X | X |
| *Leishmania gerbilli* strain LEM452 | X | X | X | X | X | X |
| *Leishmania infantum* JPCM5 | X | X | X | X | X | X |
| *Leishmania major* strain Friedlin | X | X | X | X | X | X |
| *Leishmania major* strain LV39c5 | X | X | X | X | X | X |
| *Leishmania major* strain SD 75.1 | X | X | X | X | X | X |
| *Leishmania mexicana* MHOM/GT/2001/U1103 | X | X | X | X | X | X |
| *Leishmania panamensis* MHOM/COL/81/L13 | X | X | X | X | X | X |
| *Leishmania tarentolae* Parrot-TarII | X | X | X | X | X | X |
| *Leishmania tropica* L590 | X | X | X | X | X | X |
| *Leishmania turanica* strain LEM423 | X | X | X | X | X | X |
| *Leptomonas pyrrhocoris* H10 | X | X | X | X | X | X |
| *Leptomonas seymouri* ATCC 30220 | X | X | X | X | X | X |
| *Trypanosoma brucei brucei* TREU927 | X | X | X | X | X | X |
| *Trypanosoma brucei gambiense* DAL972 | X | X | X | X | X | X |
| *Trypanosoma brucei* Lister strain 427 | X | X | X | X | X | X |
| *Trypanosoma congolense* IL3000 | X | X | X | X | X | X |
| *Trypanosoma cruzi* CL Brener Esmeraldo-like | X | X | X | X | X | X |
| *Trypanosoma cruzi* CL Brener Non-Esmeraldo-like | X | X | | X | X | X |
| *Trypanosoma cruzi* Dm28c | X | X | X | X | X | X |
| Trypanosoma cruzi JR cl. 4 | | | | | | |
| *Trypanosoma cruzi marinkellei* strain B7 | X | X | X | X | X | X |
| *Trypanosoma cruzi* strain CL Brener | | | | | | |
| *Trypanosoma cruzi* strain Esmeraldo | | | | | | |
| *Trypanosoma cruzi* Sylvio X10/1 | X | X | X | | | X |
| *Trypanosoma cruzi* Tula cl2 | | | | | | |
| *Trypanosoma evansi* strain STIB 805 | X | X | X | X | X | X |
| *Trypanosoma grayi* ANR4 | X | X | X | X | X | X |
| *Trypanosoma rangeli* SC58 | | X | X | X | X | X |
| *Trypanosoma vivax* Y486 | X | X | X | X | X | X |
| unclassified Leishmania Leishmania sp. MAR LEM2494 | X | X | X | X | X | X |

**Table S2: Primers**

| Construct | | |
|---|---|---|
| p166RNAi | FWD | 5'-**GGGGACAAGTTTGTACAAAAAAGCAGGCT** TCTTGCGCACATCTCTGGTT-3' |
| | RV | 5'-**GGGGACCACTTTGTACAAGAAAGCTGGGT** TTGCCAAGTGAACTGTTGCG-3' |
| p197RNAi | FWD | 5'-AGTCG **AAGCTTGGATCC**AAGAGGATGAGCGGCGGCTA-3' |
| | RV | 5'-TCCGA**TCTAGACTCGAG**ACGGAGAGA AAGAGGCACAA-3' |
| p166PTP | FWD | 5'-TA**GCGGCCGC**TTCTGGTCTGACTTCACACAAC-3' |
| | RV | 5'-TA**GGGCCC**ATGTAGCAACCTCAACACG-3' |
| p197PTP | FWD | 5'-A**GGGCCC**TTTAAGTGTGGAGAGTCTGC-3' |
| | RV | 5'-TA**CGGCCG**TAGAATTACCCGGTCCGCTAC-3' |

**Table S3: Antibodies**

| **Primary antibodies** | | IF | WB | |
|---|---|---|---|---|
| BBA4 | mouse | 1:100, 1:200 | | (1) |
| Mab22 | mouse | 1:10 | | (2) |
| PAP | | | 1:1000 or 1:2000 | Sigma |
| α- ATOM40 | rabbit | | 1:10000 | (3) |
| α- ef-1 alpha | mouse | | 1:10000 | Santa Cruz |
| α- HA | rat | 1:1000 | | Sigma |
| α- HA | rabbit | 1:1000 | 1:1000 | Sigma |
| α- myc | rabbit | 1:1000 | 1:1000 | Sigma |
| α- myc | mouse | 1:50 | 1:1000 | Sigma |
| α- Protein A | rabbit | 1:1000, 1:2000 | | Sigma |
| α- TAC102 | rat | 1:1000 | 1:10000 | (4) |
| α- TAC102 | mouse | 1:1000, 1:2000 | 1:1000 | (4) |
| α- TAC60 | rabbit | 1:50 | | (5) |
| YL1/2 | rat | 1:200, 1:100000 | | (6) |
| **Secondary antibodies** | | | | |
| Alexa Fluor 488 goat anti-mouse IgG (H+L) | | 1:1000 | | Invitrogen |
| Alexa Fluor 488 goat anti-rabbit IgG | | 1:1000 | | Invitrogen |
| Alexa Fluor 488 goat anti-rat IgG | | 1:500, 1:1000 | | Life technologies |
| Alexa Fluor 594 goat anti-mouse IgG (H+L) | | 1:1000 | | Molecular Probes |
| Alexa Fluor 594 goat anti-rabbit IgG (H+L) | | 1:1000 | | Life technologies |
| Alexa Fluor 594 goat anti-rat IgG | | 1:1000 | | Invitrogen |
| Alexa Fluor 647 goat anti-rat IgG (H+L) | | 1:1000 | | Life technologies |
| rabbit α- mouse HRP-conjugated | | | 1:10000 | Dako |
| rabbit anti-rat HRP-conjugate | | | 1:10000 | Dako |
| swine anti-rabbit HRP-conjugate | | | 1:10000 | Dako |
| goat anti-rabbit 680 LT | | | 1:10000 | LI-COR |

## References


1. Woods A, et al. (1989) Definition of individual components within the cytoskeleton of Trypanosoma brucei by a library of monoclonal antibodies. *J Cell Sci* 93(Pt 3):491–500.

2. Bonhivers M, Landrein N, Decossas M, Robinson DR (2008) A monoclonal antibody marker for the exclusion-zone filaments of Trypanosoma brucei. *Parasit Vectors* 1(1):21.

3. Pusnik M, et al. (2011) Mitochondrial preprotein translocase of trypanosomatids has a bacterial origin. *Curr Biol* 21(20):1738–1743.

4. Trikin R, et al. (2016) TAC102 Is a Novel Component of the Mitochondrial Genome Segregation Machinery in Trypanosomes. *PLoS Pathog* 12(5):1–27.

5. Käser S, et al. (2017) Biogenesis of a mitochondrial DNA inheritance machinery in the mitochondrial outer membrane. doi:10.1101/190751.

6. Kilmartin J V., Wright B, Milstein C (1982) Rat monoclonal antitubulin antibodies derived by using a new nonsecreting rat cell line. *J Cell Biol* 93(3):576–582.